# Cooperative Oxygen Binding, Subunit Assembly, and Sulfhydryl Reaction Kinetics of the Eight Cyanomet Intermediate Ligation States of Human Hemoglobin†

Michael L. Doyle and Gary K. Ackers*

*Department of Biochemistry and Molecular Biophysics, Washington University School of Medicine, St. Louis, Missouri 63110*

*Received February 28, 1992; Revised Manuscript Received July 30, 1992*

ABSTRACT: Correlations between the energetics of cooperativity and quaternary structural probes have recently been made for the intermediate ligation states of Hb [Daugherty et al. (1991) *Proc. Natl. Acad. Sci. US 88*, 1110–1114]. This has led to a "molecular code" which translates configurations of the 10 ligation states into switch points of quaternary transition according to a "symmetry rule"; T → R quaternary structure change is governed by the presence of at least one heme-site ligand on each of the $\alpha\beta$ dimeric half-molecules within the tetramer [see Ackers et al. (1992) *Science 255*, 54–63, for summary]. In order to further explore this and other features of the cooperative mechanism, we have used oxygen binding to probe the energetics and cooperativities for the vacant sites of the cyanomet ligation species. We have also probed structural aspects of all eight cyanomet ligation intermediates by means of sulfhydryl reaction kinetics. Our oxygen binding results, obtained from a combination of direct and indirect methods, demonstrate the same combinatorial aspect to cooperativity that is predicted by the symmetry rule. Overall oxygen affinities of the two singly-ligated species $(\alpha^{+CN}\beta)(\alpha\beta)$ and $(\alpha\beta^{+CN})(\alpha\beta)$ were found to be identical ($p_{median}$ = 2.4 Torr). In contrast, the doubly-ligated species exhibited two distinct patterns of oxygen equilibria: the asymmetric species $(\alpha^{+CN}\beta^{+CN})(\alpha\beta)$ showed very high cooperativity ($n_{max}$ = 1.94) and low affinity ($p_{median}$ = 6.0 Torr), while the other three doubly-ligated species showed diminished cooperativity ($n_{max}$ = 1.23) and considerably higher oxygen affinity ($p_{median}$ = 0.4 Torr). Extremely high oxygen affinities were found for the triply-ligated species $(\alpha^{+CN}\beta^{+CN})(\alpha\beta^{+CN})$ and $(\alpha^{+CN}\beta^{+CN})(\alpha^{+CN}\beta)$ ($p_{median}$ = 0.2 Torr). Their oxygen binding free energies are considerably more favorable than those of the $\alpha$ and $\beta$ subunits within the dissociated $\alpha\beta$ dimer, demonstrating directly the quaternary enhancement effect, i.e., enhanced oxygen affinity at the last binding step of tetramer relative to the dissociated protomers. Oxygen binding free energies measured for the $\alpha$ subunit within the isolated $(\alpha\beta^{+CN})$ dimer and for the $\beta$ subunit within the isolated $(\alpha^{+CN}\beta)$ dimer sum to the free energy for binding two oxygens to normal hemoglobin dimers (−16.3 ± 0.2 versus −16.7 ± 0.2, respectively), arguing against cooperativity in the isolated dimer. Correlations were established between cooperative free energies of the 10 cyanomet ligation microstates and the kinetics for reacting their free sulfhydryl groups. The kinetics were resolved into four distinct patterns (presumably corresponding to distinct allosteric structures) as follows: (1) deoxy; (2) $(\alpha^{+CN}\beta)(\alpha\beta)$, $(\alpha\beta^{+CN})(\alpha\beta)$, and $(\alpha^{+CN}\beta^{+CN})(\alpha\beta)$; (3) $(\alpha^{+CN}\beta)(\alpha\beta^{+CN})$, $(\alpha^{+CN}\beta)_2$, $(\alpha\beta^{+CN})_2$, $(\alpha^{+CN}\beta^{+CN})(\alpha\beta^{+CN})$, and $(\alpha^{+CN}\beta^{+CN})(\alpha^{+CN}\beta)$; and (4) the fully-ligated state $(\alpha^{+CN}\beta^{+CN})_2$. These results in combination with previous findings strongly support the operation of a symmetry rule which translates changes in configuration of heme-site ligation into the T → R quaternary structural transition.

A conventional approach to studying the details of Hb[1] cooperativity entails resolving populations of molecular species with a *total* of 0, 1, 2, 3, or 4 ligands bound from nonlinear regression analysis of high-precision oxygen binding isotherms [cf. Mills et al. (1976), Johnson et al. (1976) and Imai (1982)]. The extensive data bases that have been obtained from such studies impose energetic constraints that must be satisfied by any proposed mechanisms of Hb cooperativity. Nevertheless, further dissection of these composite energetic terms into contributions from the specific microscopic isomers at each ligation stoichiometry (Figure 1) is essential to understand the cooperative mechanism. Two major enigmas have precluded experimental delineation of these isomeric contributions. First, the highly cooperative nature of Hb suppresses the intermediate ligation species whose structural and energetic properties must be known. Second, the dissociation and reassembly of $\alpha\beta$ dimers and lability of the heme iron–oxygen bond have prevented isolation and investigation of the eight partially-oxygenated microstate species.

To circumvent these barriers, an experimental strategy has been developed which exploits (1) the use of cyanomet and other nonlabile heme-site "ligands" and (2) subunit assembly equilibrium measurements to determine ligation energetics of the tetrameric microstates (Smith & Ackers, 1985; Ackers & Smith, 1987; LiCata et al., 1990). The latter strategy exploits the pathway-independent virtue of thermodynamics, and conservation of energy around thermodynamic cycles of dimer–tetramer assembly and ligation (see, for example, Figure 5). These methods led to the first report of the energetics of all 10 ligation microstates of human Hb (Smith & Ackers, 1985). Evaluation of those microstate energetics, and of other nonlabile ligands (Smith et al., 1987), revealed a combinatorial aspect to the control of cooperativity in Hb (Ackers & Smith, 1987) and demonstrated clearly (Ackers, 1990) that cooperative cyanomet ligation does not conform to a two-state concerted mechanism (Monod et al., 1965). In particular, the two-state mechanism cannot accommodate the sharply contrasting energetics of the doubly-ligated microstate

† This work was supported by NIH Grants R37-GM24486 and PO1-HL4053, and by NSF Grant DMB 9107244.

* To whom correspondence should be addressed.

[1] Abbreviations: Hb, human hemoglobin; $Na_2EDTA$, disodium ethylenediaminetetraacetic acid; $O_2$, molecular oxygen; 4-PDS, 4,4′-dithiodipyridine; Tris, tris(hydroxymethyl)aminomethane.

0006-2960/92/0431-11182$03.00/0 

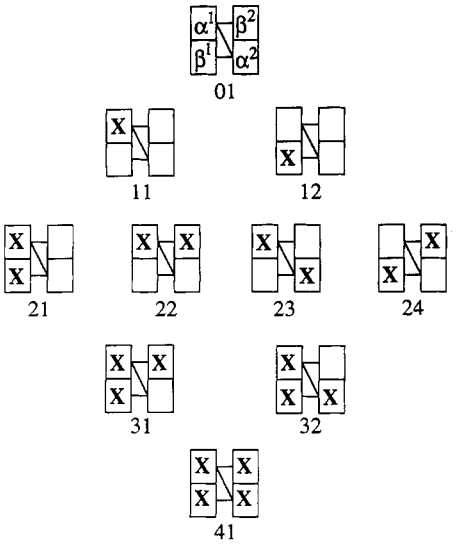


FIGURE 1: Topographical representation of the 10 ligation microstate isomers of tetrameric Hb. Subunits bound with cyanide are denoted by X. The orientation of $\alpha$ and $\beta$ subunits within the tetramer is shown in the unligated species [01]. Lines connecting the two dimeric half-molecules represent intersubunit contacts across the $\alpha^1\beta^2$ interface.

species $(\alpha^{+CN}\beta^{+CN})(\alpha\beta)$ compared to the remaining three doubly-ligated isomers (see Figure 1). Recent work on hemoglobins partially-ligated with NO has shown that the asymmetric doubly-ligated species $(\alpha^{NO}\beta^{NO})(\alpha\beta)$ (i.e., species [21]; see Figure 1 for species definitions) has considerably different subunit dissociation kinetics than the symmetric species [23] and [24] (Perrella et al., 1990a).

A subsequent step in deciphering the cooperative mechanism of Hb involves correlation of microstate ligation energetics with quaternary and tertiary structure changes. Daugherty et al. (1991) concluded from the effects of protons and single-site mutations on quaternary assembly that cyanomet species [21] adopts a quaternary structure indistinguishable from that of deoxy "T". (Here we employ the terminology "change in quaternary structure" to mean global reorientation of the dimeric half-molecules, as opposed to minor changes involving local intersubunit hydrogen bonds, etc.)

Correlations between microstate energetics and quaternary structure have recently been made for all 10 ligation states of Hb, leading to a molecular "code" for cooperativity which translates configurations of the 10 ligation states into switch points of quaternary transition [summarized in Ackers et al. (1992)]. The present study comprises a major component of that synthesis. A prominent feature is the "symmetry rule"; T→R quaternary structure change is governed by the presence of at least one heme-site ligand on each of the $\alpha\beta$ dimeric half-molecules within the tetramer. Cooperativity-linked tertiary structure changes (that is, intersubunit structure changes not involving global reorientation of dimers) were also implicated to occur within each of the two quaternary structures, T and R.

In the present study we have determined the cooperative free energy distributions that result from cyanomet ligation using $O_2$ as a probe of the vacant heme sites. Our results, using a combination of direct and indirect methods, demonstrate the same combinatorial aspect to cooperativity that is predicted by the symmetry rule. The cooperative free energy "spent" during formation of each cyanomet microstate is determined as the difference between the total cooperative free energy (expended upon binding to all four heme sites) and the free energy penalty for $O_2$ binding to the vacant heme sites on each cyanomet species.

In parallel with the oxygen equilibrium studies we have probed structural properties of the 10 microstates by measuring the kinetics of reacting free sulfhydryl groups, i.e., the $\beta$93 cysteines (Guidotti & Konigsberg, 1964). The reaction kinetics of the free sulfhydryls are known to differ widely between the deoxy and oxy ligation end states (Riggs, 1952, 1961; Benesch & Benesch, 1962). Although it is generally accepted that changes in sulfhydryl reactivity are largely due to the T to R quaternary structure transition, tertiary structure changes may also contribute (Guidotti, 1965; Perutz et al., 1974). The present sulfhydryl reactivity results provide a consistency test for the recently proposed code for Hb cooperativity and also provide a data base for dissecting the relative contributions of quaternary and tertiary structure changes in modulating sulfhydryl reactivity.

We also present new data on the magnitude of "quaternary enhancement" free energies of Hb [Mills & Ackers, 1979a,b; Gibson & Edelstein, 1987; Philo & Lary, 1990; see Ackers and Johnson (1990) for review]. That is, in addition to "quaternary constraints" which oppose $O_2$ binding to the $\alpha_2\beta_2$ tetramer relative to the isolated $\alpha\beta$ dimer (Monod et al., 1965), tetrameric Hb also exhibits enhance tetrameric $O_2$ affinity at the fourth binding step relative to that of the dissociated dimer (Mills & Ackers, 1979a). The thermodynamic linkages between subunit assembly and $O_2$ binding to triply cyanomet Hb determined in the present study allow an essentially direct measure of quaternary enhancement free energy.

Finally, the present data provide an accurate measure of the affinity difference for $O_2$ binding to the $\alpha$ and $\beta$ subunits within the isolated $\alpha\beta$ dimer. The $\alpha$ and $\beta$ subunit $O_2$ binding free energies were measured independently on $\alpha\beta$ dimers where one of the two subunits was already bound with cyanomet.

## MATERIALS AND METHODS

*Hemoglobin Preparations.* $HbA_0$ was prepared by the method of Williams and Tsay (1973). Fully cyanomet $HbA_0$ was prepared from normal $HbA_0$ by oxidation with a 1.1 molar excess of potassium ferricyanide at room temperature for 3 min, followed by reaction with potassium cyanide. The cyanomet Hb was then equilibrated against 0.1 M Tris, 0.1 M NaCl (0.18 M total chloride), 1 mM $Na_2EDTA$, and 10 $\mu$M KCN, pH 7.40 (at 21.5 °C), using CF25 Centriflo Ultrafiltration Membrane Cones (Amicon, Inc.), concentrated to 10 mM heme, and stored frozen in liquid nitrogen until use. Preparation of the symmetric doubly cyanomet species $(\alpha^{+CN}\beta)_2$ and $(\alpha\beta^{+CN})$ has been described previously (Smith & Ackers, 1985).

*Preparation of Hybrid Hemoglobins.* Six of the ten ligation microstates in Figure 1 cannot be studied in isolation due to $\alpha\beta$ dimer rearrangement reactions. However, they can be studied as hybrid mixtures in the presence of two parent species. For example, species [21] $(\alpha^{+CN}\beta^{+CN})(\alpha\beta)$ is prepared by mixing the two parent species [01] $(\alpha\beta)(\alpha\beta)$ with [41] $(\alpha^{+CN}\beta^{+CN})(\alpha^{+CN}\beta^{+CN})$. These two parent species undergo dimer rearrangement reactions that yield species [21] as a "hybrid" tetramer (see Figure 1 for nomenclature of all species) in the presence of the original parent tetramers. The approaches to and maintenance of equilibrium of the hybrid mixtures were verified by assaying the distribution of species as a function of time with cryogenic isoelectric focusing [cf. Perrella et al. (1990a) and Speros et al. (1991)]. Equilibration time for the various hybrid systems ranged from several minutes (species [22], [31], and [32]) to 40–60 h (species [11], [12], and [21]). Anaerobic conditions were

maintained enzymatically with glucose oxidase, glucose, and catalase (Sigma). The total hemoglobin concentration during incubation of the hybrid mixtures was approximately 1.5 mM in heme units.

Unlikely sources of the effects observed in this study are dissociation of $\alpha\beta$ dimers into $\alpha$ and $\beta$ subunits, or heme exchange of cyanide-bound ferric hemes and oxygenated/deoxygenated ferrous hemes. On the basis of kinetic studies (Bunn & Jandl, 1968; Mrabet et al., 1986), these systematic errors occur on a much slower time scale than the dimer–tetramer rearrnagement reactions studied here and are estimated to be less than 1% under the conditions of this study. Additional evidence against systematic errors from monomer rearrangement comes from studies of the approach to equilibrium of hybrid tetramers such as species [21]. These have been studied over a wide range of conditions (LiCata et al., 1990) and have been found to conform to an analytic model for dimer–dimer rearrangement.

A further possibility is that of valency exchange which might transform some of the species [21] into singly-ligated, or triply-ligated, forms, also producing species [23] and [24] by disproportionation. We have found that these effects, which are easily detected by measurements of dissociation kinetics [see Perella et al. (1990a)] are suppressed to an immeasurably low level by the presence of 10 $\mu$M KCN, as employed in this study.

*Dimer–Tetramer Assembly by Analytical Gel Chromatography.* Assembly equilibria for the deoxy and oxy forms of the doubly-ligated cyanomet species [23] and [24] were measured by analytical gel chromatography (Ackers, 1970; Valdes & Ackers, 1979) using Sephadex G-100 (Sigma Corp.). Elution volumes $V_{el}$ at specific total Hb concentrations were determined from "large-zone" elution profiles as equivalent sharp boundaries on leading and trailing edges. The equivalent sharp boundaries were measured as centroids, either by planimetry (deoxy Hbs) or by numerical integration (oxy Hbs). For a dimer–tetramer associating macromolecule, the elution volume at a given Hb concentration depends on the fractions of dimers and tetramers and their elution volumes, $V_D$ and $V_T$, respectively, as

$$V_{el} = V_D f_D + V_T f_T \tag{1}$$

Here the fraction $f_D$ of Hb as dimers is

$$f_D = \frac{-1 + \sqrt{1 + 4K_2P_t}}{2K_2P_t} \tag{2}$$

where $P_t$ is total heme concentration and $K_2$ is the dimer–tetramer association equilibrium constant. The fraction as tetramers is $1 - f_D$. The elution volume data were fitted by nonlinear regression according to eq 1. After regression, the data were illustrated in terms of the weight-average partition coefficient $\bar{\sigma}_w$:

$$\bar{\sigma}_w = \frac{V_{el} - V_0}{V_i} \tag{3}$$

where $V_0$ and $V_i$ are the void and included volumes (9.45 and 20.56 mL, respectively). Included and void volumes were measured from "small-zone" experiments on the nonassociating molecules glycylglycine ($V_{el}$ = 30.01 mL) and blue dextran ($V_0$ = 9.45 mL). The column flow rate was maintained at 14.40 ± 0.05 mL h$^{-1}$ with an LKB 10200 Perpex pump.

Dimer–tetramer assembly free energies for the deoxygenerated species were measured by anaerobic analytical gel chromatography. Anaerobicity was achieved with a Coy Laboratory Products Type B anaerobic chamber equipped with three catalyst boxes. Oxygen partial pressure inside the chamber was monitored continually with a Coy Model 10 gas analyzer and never exceeded the 1 ppm detection limit of the analyzer. Eluant buffer was deoxygenated exhaustively by rapid stirring inside the anaerobic chamber for approximately 48 h. Deoxygenation of species [23] and [24] was carried out by gentle shaking of the samples under a flow of $O_2$-free nitrogen for 45 min at 4 °C and verified spectrophotometrically in the visible region. Elution profiles of the deoxy Hbs were monitored inside the chamber with a Shimadzu UV-150-02 spectrophotometer. Dimer–tetramer assembly free energies of fully-oxygenated species were measured under a gaseous atmosphere of air with a Cary 4 spectrophotometer as the column monitor. Temperature was maintained at 21.5 °C for all analytical gel chromatography experiments with a Lauda K-2/R thermoregulator (Brinkmann Instruments).

*$O_2$ Binding Equilibria.* A thin-layer spectrophotometric technique (Dolman & Gill, 1978) was used to measure $O_2$ binding curves for the following reasons: First, the thin-layer cell allows detailed shape analysis of isotherms of high-oxygen-affinity Hbs, which would be difficult or impossible to achieve with high-precision $O_2$ electrode-based systems [cf. Doyle and Ackers (1992)]. Second, very high concentrations of Hb can be studied, facilitating resolution of the energetics corresponding to tetramers (although dimers were included in the partition function). Third, the Gill cell is gentler on the Hb sample than conventional methods which employ mechanical stirring procedures rather than rapid diffusion from a thin layer. Gentle treatment of partially-oxygenated cyanomet Hb intermediates is important because there is an increased tendency to oxidize relative to normal Hb. Typical degradation of the partially cyanomet Hbs during $O_2$ equilibrium measurements with the thin-layer cell was approximately 5% as judged by base-line drift.

Approximately 8 $\mu$L of Hb was assembled into a 0.005-cm path length thin layer. The thin layer was connected to a high-precision gas-dilution chamber and equilibrated with an atmosphere of humidified 3.48% $O_2$ (Matheson Gas Co. certified standard, balance nitrogen). Hb was deoxygenated by dilution of the $O_2$ partial pressure with humidified $O_2$-free nitrogen gas (Scott Specialty Gases). Each dilution in the initial $O_2$ partial pressure, $X_{i-1}$, to the final value, $X_i$, is given by

$$X_i = X_{i-1}D \tag{4}$$

where $D$ is an adjustable logarithmic dilution factor, equal to 0.5855 (±0.0010) in the present study. Concomitant changes in fractional saturation were monitored at 415 nm with a Cary 3 spectrophotometer. Temperature was maintained at 21.5 °C with a Tronac 1040 precision temperature controller and calibrated with a surface thermistor (YSI 427) epoxied to the surface of the thin-layer sample cell with high thermally conductive epoxy (Omegabond 101, Omega Engineering, Inc.).

Data obtained with the thin-layer cell were analyzed according to the general fitting equation:

$$\Delta A(i) = \Delta A_T[\bar{Y}(X_{i-1}) - \bar{Y}(X_i)] \tag{5}$$

The observed change in absorbance due to the $i$th dilution in $O_2$ partial pressure (or equivalently activity) from $X_{i-1}$ to $X_i$ is $\Delta A(i)$, and the total absorbance change for complete oxygenation is $\Delta A_T$. Fractional $O_2$ saturation functions, $\bar{Y}$, for each of the partially-ligated cyanomet Hbs are derived in the appendix. Free energies are reported with 1 M $O_2$ as the reference concentration and are based on conversion from partial pressures to molarities with the Henry's Law constant $1.78 \times 10^{-6}$ M Torr$^{-1}$ (Wilhelm et al., 1977). All data were analyzed by the nonlinear least-squares program NONLIN

(Johnson & Frasier, 1985) on a Hewlett-Packard 9000/835 computer, with equal weighting on each data point.

In order to illustrate the Gill cell data (Figures 4 and 7), there is a somewhat arbitrary choice for allocation of the observed absorbance changes along the abscissa. Namely, the measured $\Delta A(i)$ values may be plotted anywhere between the initial and final $O_2$ partial pressures of each dilution step. The logical plotting location is at the geometric mean of the two partial pressures, $\xi_i = (X_i X_{i-1})^{1/2}$, since the data approximate the first derivative of the isotherm at $\xi_i$ (Di Cera & Gill, 1988).

*Kinetics for Reacting Free Sulfhydryls.* The kinetics of reacting free sulfhydryl groups with 4,4′-dithiodipyridine (4-PDS) were monitored spectrophotometrically at 324 nm as the appearance of 4-thiopyridone (Ampulski et al., 1969). Reactions with species [11], [12], and [21] (Figure 1) required preincubations of 50–100 h to reach equilibrium. Kinetics of these species were measured at 25–29 °C with an Applied Photophysics RX.1000 stopped-flow apparatus equipped with a Cary 3 spectrophotometer. The dead time of this setup originated from a 33-ms data acquisition period of the spectrophotometer used. These stopped-flow kinetics measurements were performed inside the Coy anaerobic chamber.

Sulfhydryl reactions at 21.5 °C, and with the remaining species, were initiated by inversion of a glass-stoppered split-cell cuvette and monitored with a Cary 4 spectrophotometer. The "dead time" was 10–15 s. Deoxygenation of the reactants was performed inside the anaerobic chamber. Sample integrity was verified spectrally in the visible region after each experiment. Temperature for the split-cell data was maintained at 21.5 °C with a Brinkmann Instruments Lauda K-2/R thermoregulator. The optical path length for all kinetic experiments was 0.9 cm.

## RESULTS

*$O_2$ Binding Energetics of Species [11] and [12].* Resolution from $O_2$ equilibrium curves of the stepwise $O_2$ binding free energies for the vacant sites of cyanomet species [11] and [12] is complicated by the fact that these species must be studied as hybrid mixtures in the presence of the highly-cooperative parent species [01] and a second, moderately-cooperative parent species (either [23] or [24]). In principle, this problem might be approached by global analysis of an extensive set of $O_2$ binding curves, i.e., fractional saturation as a function of (1) $O_2$ activity, (2) relative proportions of the parent species, and (3) total Hb concentration. In practice, however, simultaneous resolution of the binding properties of all these cooperative tetramers in mixture is untenable. Considerable difficulty is encountered even in resolving the four $O_2$ binding free energies of the isolated parent species [01] [cf. Mills et al. (1976) and Chu et al. (1984)]. In addition, the hybridization reactions for singly-ligated species contain very slow kinetic components (Philo, 1992; Daugherty & Ackers, 1992) that greatly complicate the use of direct $O_2$ binding strategies for these species.

On the other hand, the $O_2$ affinities (or $p_{median}$ values) of the vacant sites on species [11] and [12] can be determined accurately and rigorously from subunit assembly measurements conducted at equilibrium using simple conservation of free energy. Figure 2 shows the thermodynamic linkage between two sets of hybridization equilibria of species [11] corresponding to the deoxygenated and fully-oxygenated states (I and II, respectively). Each of the hybridization equilibria

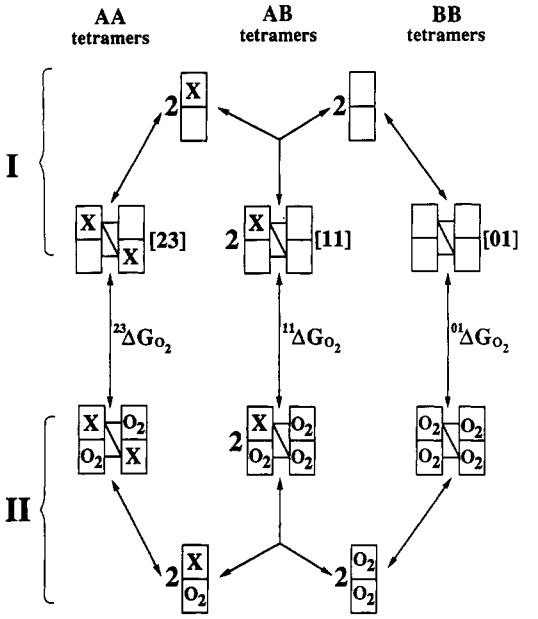


FIGURE 2: Thermodynamic linkage scheme for determination of the free energy $^{11}\Delta G_{O_2}$ of $O_2$ binding to the three vacant hemesites of species [11]. Tetramers are shown as two dimeric half-molecules with connections at the "$\alpha^1\beta^2$ interface" (see Figure 1 for orientation). Dissociated $\alpha\beta$ dimers are represented with $\alpha$ subunits on top. The upper and lower portions of the linkage scheme correspond to individual hybridization experiments performed anaerobically (I) and under fully-oxygenated conditions (II). The "hybrid" Hb AB is formed by dimer rearrangement reactions between the parent species AA and BB. The $O_2$ binding free energies $^{23}\Delta G_{O_2}$ and $^{01}\Delta G_{O_2}$ of species [23] and [01], respectively, were measured independently by $O_2$ equilibrium measurements (see text).

were analyzed in terms of the deviation free energy $\delta$:

$$\delta = -RT \ln \frac{f_{AB}}{2\sqrt{f_{AA} f_{BB}}} \tag{6}$$

where the $f$ terms are equilibrium fractions of AA, AB, and BB tetramers (A and B represent the two types of parent $\alpha\beta$ dimers). These fractions were measured from direct optical scanning of cryogenic isoelectric focusing gels (LiCata et al., 1990) which reflect the species distributions in an incubation mixture at 21.5 °C. The deviation free energy $\delta$ pertains to free energies of the three tetrameric species only (dimer free energies cancel):

$$\delta = G_{tet}^{AB} - \frac{1}{2}(G_{tet}^{AA} + G_{tet}^{BB}) \tag{7}$$

where terms on the right denote chemical potentials of tetramers relative to any appropriate reference state [see LiCata et al. (1990) for derivation of eqs 6 and 7 and further experimental details]. This relation (eq 7) holds rigorously for the deoxy scheme, $\delta_I$, and separately for the oxy scheme, $\delta_{II}$, of Figure 2. By conservation of energy, the difference between the two is related to the overall $O_2$ binding free energies of the three tetramers as

$$\delta_{II} - \delta_I = {}^{11}\Delta G_{O_2} - \frac{1}{2}({}^{23}\Delta G_{O_2} + {}^{01}\Delta G_{O_2}) \tag{8}$$

The $^{ij}\Delta G_{O_2}$ free energies correspond to fully oxygenating the vacant sites on species [$ij$]. Experimental values were as follows: $\delta_{II} = 0.01 \pm 0.08$ kcal and $\delta_I = 0.06 \pm 0.1$ kcal from cryogenic isoelectric focusing, and $^{23}\Delta G_{O_2} = -16.47 \pm 0.05$ kcal and $^{01}\Delta G_{O_2} = -27.1 \pm 0.2$ kcal from direct $O_2$ binding experiments (conducted separately). Substituting these values into eq 8 and solving for $^{11}\Delta G_{O_2}$, we obtain a value of $-21.7 \pm 0.3$ kcal/3 mol of $O_2$ for the free energy of oxygenating the vacant sites of species [11]. Similarly, the $O_2$ binding free

Table I: $O_2$ Binding Parameters for Vacant Sites of Tetrameric Cyanomet Ligation Species of Hb[a]

| species *ij* | $p_{median}$ (Torr) | $^{ij}\Delta G_{O_2}$ | method[c] | sites | $^{ij}\Delta G_{O_2}$/ sites | Hill $n_{max}$ |
|---|---|---|---|---|---|---|
| [01][b] | 5.3 ● 0.4 | −27.1 ± 0.2 | B, P | 4 | −6.78 | 3.38 |
| [11] | 2.58 ± 0.55 | −21.7 ± 0.3 | A, H | 3 | −7.23 | 1.79[d] |
| [12] | 2.20 ± 0.47 | −21.9 ± 0.3 | A, H | 3 | −7.30 | 1.78[d] |
| [21] | 6.0 ± 1.8 | −13.4 ± 0.3 | A, H | 2 | −6.70 | 1.94[e] |
| [22] | 0.38 ± 0.06 | −16.64 ± 0.13 | A, H | 2 | −8.32 | 1.00[f] |
| [23] | 0.44 ± 0.03 | −16.47 ● 0.05 | B, P | 2 | −8.24 | 1.23 |
| [24] | 0.47 ± 0.03 | −16.39 ± 0.05 | B, P | 2 | −8.20 | 1.23 |
| [31] | 0.18 ± 0.04 | −8.74 ± 0.10 | A, H | 1 | −8.74 | 1.00 |
| [32] | 0.23 ± 0.04 | −8.62 ± 0.10 | A, H | 1 | −8.62 | 1.00 |
| [41] | n.a. | n.a. | n.a. | 0 | n.a. | n.a. |
| $\alpha\beta$, dimer[b] | 0.36 ● 0.07 | −16.7 ± 0.2 | B, P | 2 | −8.35 | 1.00 |

[a] Conditions as in Figure 3. See Figure 1 for microstate species designations. [b] Chu et al., 1984. [c] Symbols B and A denote approaches of direct $O_2$ binding and linkage to dimer–tetramer assembly, respectively. P and H denote respectively whether the studies were on pure tetrameric species or hybrid mixture. [d] Hill slopes were modeled from combinations of cyanomet and $O_2$ binding equilibrium constants (see text). [e] The free energy for binding the last $O_2$ to species [21] was calculated from the measured values of the species [31] and [32]. [f] Within standard error this value may be as high as 1.31. n.a., not applicable.

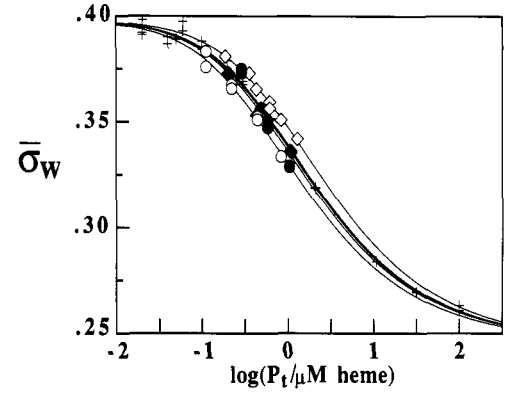


FIGURE 3: Analytical gel chromatography weight-average partition coefficient versus logarithm of Hb concentration for normal oxy Hb (+), oxy (●) and deoxy (○) species [23], and oxy (◆) and deoxy (◇) species [24]. Two data points are plotted for each Hb and at each concentration that correspond to the leading and trailing edges of each "large-zone" experiment. Curves represent global-analysis best-fit parameters for the dimer–tetramer equilibria of each Hb (parameters in text). The asymptotic dimer and tetramer partition coefficients were 0.398 and 0.246, respectively. Conditions: 0.1 M Tris, 0.1 M NaCl (0.18 M total chloride), 1 mM $Na_2EDTA$, and 10 μM KCN, pH 7.40 at 21.5 °C.

energy for species [12] was found to be $^{12}\Delta G_{O_2} = -21.9 \pm 0.3$ kcal/3 mol of $O_2$. ($\delta_{II} = 0.01 \pm 0.07$ kcal, $\delta_I = -0.1 \pm 0.1$ kcal, and $^{24}\Delta G_{O_2} = -16.39 \pm 0.05$ kcal.) $\delta_I$ values are from Perrella et al. (1990a), and $^{01}\Delta G_{O_2}$ is from Chu et al. (1984). It is noteworthy that eq 8 is rigorously independent of the $O_2$ binding free energies of the dissociated dimers.

Since Hill coefficients[2] for the sequential $O_2$ binding reactions of cyanomet species [11] and [12] were not amenable to direct measurement (above), they were calculated from experimental values of the overall $O_2$ binding free energies. The maximum Hill slopes for $O_2$ binding to the vacant heme sites of species [11] and [12] in Table I are thus apparent values, reflecting both $O_2$ and cyanomet ligation free energies. For instance, the free energy for the cyanomet ligation process [11] → [21] corrected for statistical degeneracy is equal to the difference between total $O_2$ binding free energies of species [11] and [21]. The first cyanomet binding constant to species [11] may therefore be predicted from the equilibrium constants for all three ligation pathways: [11] → [21], [11] → [22], and [11] → [23]. Modeling of the second and third $O_2$ binding equilibrium constants to species [11] was based on actual $O_2$ binding constants measured experimentally with the doubly cyanomet species (Figure 5).

*$O_2$ Binding and Dimer–Tetramer Assembly Equilibria of Species [21].* The free energy of $O_2$ binding to the vacant sites of cyanomet species [21] was determined by a procedure analogous to that described above for species [11] and [12]; that is, the thermodynamic distance between cyanomet species [21] with and without two oxygens bound on the opposite dimer was measured along subunit assembly and ($\alpha\beta$) dimer $O_2$ binding pathways. For the case of the species [21] hybridization equilibria (analogous to Figure 2), one of the parent species is [41] (fully cyanomet Hb) so that the free energy $^{41}\Delta G_{O_2}$ in going from state I to state II is zero. Experimental values for the remaining parameters of the species [21] analog of eq 8 were $^{01}\Delta G_{O_2} = -27.1 \pm 0.2$ kcal (Chu et al., 1984), $\delta_I = 0.12 \pm 0.08$ kcal (Perrella et al., 1990a), and $\delta_{II} = 0.05 \pm 0.02$ kcal. The value of $\delta_I$ is corroborated by the deoxygenated dimer–tetramer assembly free energy of species [21] determined by haptoglobin kinetics (−11.4 ± 0.1 kcal; Smith & Ackers, 1985) that leads to $\delta_I = 0 \pm 0.2$ kcal. The overall free energy for binding $O_2$ to species [21] is therefore −13.4 ± 0.3 kcal/2 mol of $O_2$ ($p_{median}$ value of 6.0 ± 1.8 Torr).

Direct $O_2$ binding experiments were also carried out on species [21] (Figure 4A). This species was necessarily in a hybrid mixture with parent species cyanomet [41] and [01]. Initial concentrations of species [41] and [01] were 4.65 and 0.169 mM heme, respectively. Under these conditions the shape of the $O_2$ equilibrium curve is dominated (approximately 95%) by species [21], so that resolution of the pertinent $O_2$ binding equilibria is, in principle, straightforward. However, the accuracy of these $O_2$ equilibrium results was questionable for two reasons. (1) The analytic model used during regression analysis (analogous to eq A5) failed to describe the data as judged by large systematic trends in the residuals (Figure 4A) and an apparent Hill slope of species [21] equal to 2.0 (corresponding to infinite cooperativity). Similar results were found using initial parent Hb concentrations of [41] = 4.63 mM and [01] = 0.337 mM heme (not shown). (2) The overall free energy difference between cyanomet species [21] with and without two oxygens bound as determined by $O_2$ equilibrium methods (−14.7 ± 0.2 kcal) was considerably more favorable than the value measured above by subunit assembly methods (−13.6 ± 0.2 kcal) [in addition to values of −13.6 ± 0.2 and −13.5 ± 0.2 kcal estimated from previously reported subunit assembly measurements of cyanomet Hbs (Smith & Ackers, 1985; Perrella et al., 1990a)]. The apparent $O_2$ binding equilibrium constant was therefore 58-fold larger than expected (apparent $p_{median}$ = 1.9 Torr).

These $O_2$ binding results are consistent with earlier studies which found $p_{median}$ = 1.7 Torr for species [21] (Imai, 1982). However, the accuracy of direct $O_2$ equilibrium studies on hybrid mixtures containing cyanomet species [21] remains questionable in view of unusual kinetic effects that have been encountered with species [21] in the measurement of subunit equilibria. In subunit assembly studies of the approach to equilibrium (LiCata et al., 1990; Johnson, 1990; M. A. Daugherty and G. K. Ackers manuscript in preparation) it was found that the anaerobic form of cyanomet species [21] required approximately 40 h. These slow rates of approach to equilibrium would not be detected by $O_2$ equilibrium

[2] The Hill slope is the first derivative of the Hill plot and represents the variance of the distribution of intermediate ligation species relative to that of a noncooperative case [cf. Edsall and Gutfruend (1983)]. A Hill slope greater than unity corresponds to favorable cooperative interactions between binding sites.

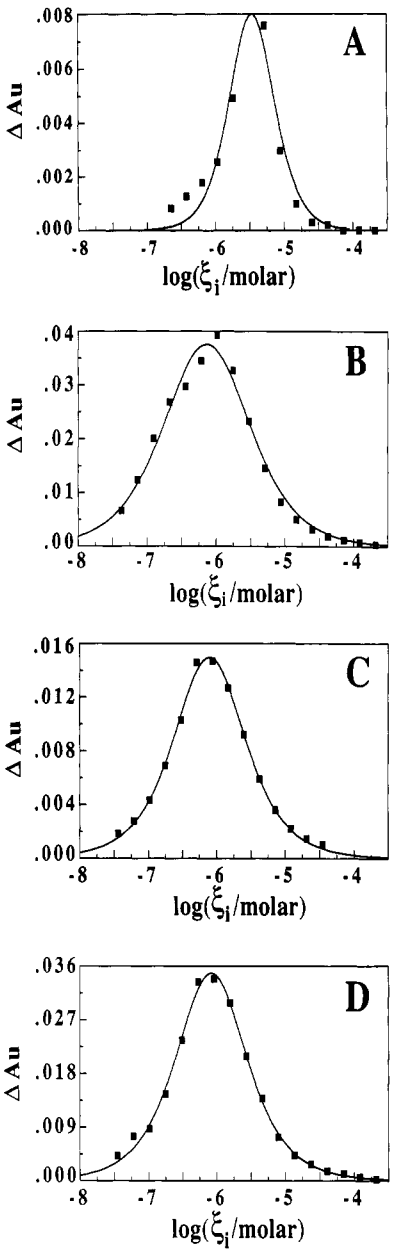


FIGURE 4: Derivative $O_2$ equilibrium isotherms (at 415 nm) for the doubly-ligated cyanomet species: (A) species [21] (in mixture with [01] and [41]), (B) species [22] (in mixture with [23] and [24]), (C) pure species [23], and (D) pure species [24]. Conditions: 0.1 M Tris, 0.1 M NaCl (0.18 M total chloride), 1 mM $Na_2EDTA$, and 10 $\mu$M KCN, pH 7.40 at 21.5 °C. Initial heme concentrations of parent species were as follows: (A) 4.63 mM species [41] and 0.337 mM species [01] and (B) 1.59 mM species [23] and 1.61 mM species [24]. Heme concentrations in (C) and (D) were 990 $\mu$M and 3.85 mM, respectively. Curves represent nonlinear regression to eq 5. The square root of the variance ($\bar{Y}$ units) was 0.0188 (A), 0.0065 (B), 0.0032 (C), and 0.0040 (D).

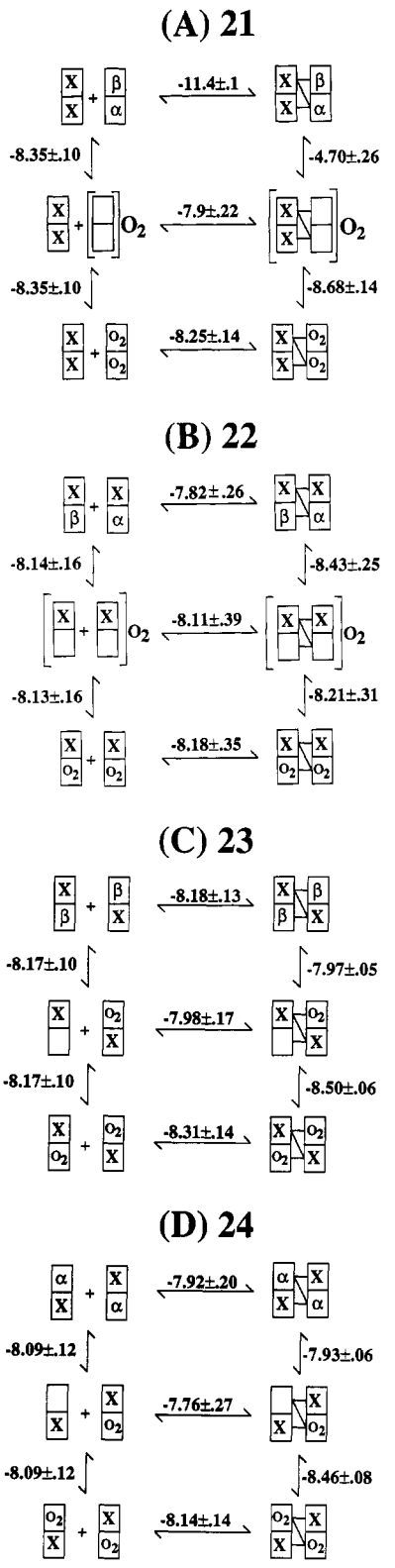


FIGURE 5: Thermodynamic linkage between dimer–tetramer assembly and $O_2$ binding to the doubly-ligated cyanomet species [21], [22], [23], and [24]. The ligand cyanomet is denoted by X. Orientation of $\alpha$ and $\beta$ subunits within the dimer and tetramer is indicated in the deoxy species. Dimer oxygenation free energies in (B) are statistical averages of the two types of dimers. Intrinsic free energies (kcal) were determined from the data in Figures 3 and 4. Conditions are given in Figure 4.

experiments (which are completed in about 1 h), but may alter both shape and affinity characteristics of the $O_2$ binding curves. The discrepancy between the subunit assembly pathway of determining the overall $O_2$ binding free energy of species [21] and the $O_2$ binding pathway also suggests that the system may not have been at equilibrium during the time course of the latter experiments. In spite of this discrepancy it is of interest that both methods yield results on the $O_2$ binding properties of species [21] that are in sharp contrast with the $O_2$ binding properties of any of the other doubly-ligated configurational isomers (determined below).

The two stepwise $O_2$ binding free energies of cyanomet species [21] (Figure 5A) were modeled from the overall $O_2$ binding energetics determined above, together with the free energies measured below for the last $O_2$ binding step of species [31] and [32]. The underlying assumption is that binding the first ligand onto the vacant heme sites of cyanomet species [21] produces the same allosteric response whether it is $O_2$ or cyanomet. This assumption is strongly supported by (1)

the energetic equivalence (±0.1 kcal) of the last $O_2$ binding free energies for species [23] and [24] (Figure 5) compared to those of species [31] and [32] (Figure 8) and (2) the fact that all determinations in the present study of the free energy of binding the fourth $O_2$ are quite similar [and also consistent with that of normal $HbA_0$ (–9.16 ± 0.35; Chu et al., 1984)]. Thus the last $O_2$ binding step to Hb is relatively insensitive to the nature and configuration of the first three heme-site ligands. Figure 5A shows the dimer–tetramer assembly and $O_2$ binding energetics of species [21] using the species [31] and [32] $O_2$ binding free energies for the last binding step. The maximum Hill slope of 1.94 for $O_2$ binding to cyanomet species [21] reveals a remarkable degree of cooperativity. (If one allows for a ±0.5 kcal error on the assumed $O_2$ binding free energy value for the last step, the range of calculated Hill slopes is 1.86–1.97.)

*Dimer–Tetramer Assembly Equilibria of Species [23] and [24].* Figure 3 shows the results of "large-zone" analytical gel permeation chromatography experiments on the oxy and deoxy forms of species [23] and [24]. Given that resolution of the assembly equilibrium constant is based on a fitting equation (eq 1) which requires the asymptotic elution volumes (or partition coefficients) of the pure dimer and tetramer forms, our approach involved independent determination of these asymptotic parameters using normal oxy Hb since its assembly free energy is known to high accuracy. Thus, in principle, once the asymptotic parameters are known, the dimer–tetramer assembly free energy of a given Hb can be determined from a single large-zone experiment. In practice, we measured elution profiles at three or more Hb concentrations for each species to verify that the samples were behaving according to the dimer–tetramer stoichiometry (as judged by consistency with shapes of best-fit curves in Figure 3 and by the shapes of the individual large-zone profiles). The reported dimer–tetramer assembly free energies for species [23] and [24] (Figure 5) were determined by global regression analysis to eq 1 and included the oxy normal Hb data in order to obtain the common parameters $V_D$ and $V_T$. Confidence intervals reported in Figure 5 thus include the uncertainty from "floating" $V_D$ and $V_T$ during regression analysis. The best-fit values of $V_D$ and $V_T$ were 17.63 and 14.51 mL, respectively. The best-fit dimer–tetramer assembly free energy for oxy normal Hb was –8.11 ± 0.14, in good agreement with a previously reported value of –8.05 ± 0.1 kcal (Chu et al., 1984). Data in Figure 5 for the deoxygenated form of species [24] are from the temperature-dependence studies of Y. Huang and G. K. Ackers (manuscript in preparation).

*$O_2$ Binding Equilibria of Species [23] and [24].* Oxygen binding experiments with species [23] and [24] are the most straightforward of all the partially-ligated cyanomet species since they can be studied in isolation. The relevant partition function therefore includes just the dimer and tetramer forms and an equilibrium constant relating the two (eq A2). Figure 4 shows $O_2$ binding equilibria of these systems measured at high Hb concentrations where tetramers dominate the shape of the isotherm. Thus it was possible to constrain the deoxygenated subunit assembly free energy during regression analysis without inducing bias error. In fact, the fitting procedure was insensitive to any reasonable constrained estimate for this parameter [perturbation by ±0.5 kcal (several times the standard deviation) led to perturbations in the first and second $O_2$ binding free energies of only ±0.02 and ±0.01 kcal]. The resulting least-squares determination of $O_2$ binding energetics for species [23] and [24] are summarized in Figure 5 and Table I. Resolution of the stepwise $O_2$ binding free energies of these species was robust by virtue of the low cooperativity of the isotherms.

The $O_2$ binding affinities and cooperativities determined in the present study, where $O_2$-linked dimer–tetramer equilibria were explicitly accounted for, agree well with previous studies which analyzed $O_2$ binding isotherms according to binding functions that did not include the $O_2$ binding properties of dimers (Maeda et al., 1972; Nagai, 1977). This agreement is not surprising given the particular values of the dimer–tetramer assembly free energies of cyanomet species [23] and [24], the low $O_2$ binding cooperativities of the isotherms, and the fact that the overall tetrameric $O_2$ affinities are nearly the same as those of the constituent dimers (Table I).

*$O_2$ Binding Equilibria of Species [22].* Species [22] must be investigated as a hybrid mixture in the presence of parent species [23] and [24]. In principle, the dimer–tetramer assembly and $O_2$ binding equilibria of all three doubly-ligated species could be resolved through a global analysis of multiple isotherms measured over a range of Hb concentrations at varying proportions of the parent species. The relevant saturation function is analogous to eq A5.

Instead, we have measured the isotherm at a single very high concentration on a mixture containing approximately 50% as species [22] and 25% each of species [23] and [24]. Since the dimer exchange between all three tetramers is rapid ($t_{1/2}$ in seconds), equilibrium is reached throughout measurement of the $O_2$ binding curve (typically 5–10-min equilibration time at each $O_2$ partial pressure). Parameters for species [23] and [24] (determined above) were constrained during regression so that only the $O_2$ binding parameters of species [22] were adjustable. The assembly free energy of species [22] was calculated from the assembly free energies of species [23] and [24] (above) together with the deviation free energy measured by Perrella et al. (1990a). Figure 4C shows the isotherm of the hybrid mixture of species [22], [23], and [24]. The results (Figure 5 and Table I) show that the overall $O_2$ affinity of species [22] is well-resolved and is essentially identical with that of species [23] and [24]. Stepwise $O_2$ binding free energies on the other hand were poorly resolved, due to the necessity of studying species [22] as a hybrid mixture.

Studies on chemically cross-linked species [22] (Miura et al., 1987) yielded a maximum $O_2$ binding Hill slope of 1.2, suggesting that a small amount of cooperativity may exist in the un-cross-linked species [22] but not detected in the $O_2$ binding measurements of the hybrid mixture. Given the standard errors on the stepwise $O_2$ binding free energies of species [22], the maximum Hill slope may be as high as 1.3.

*$O_2$ Binding and Assembly Equilibria of Species [31] and [32].* Species [31] and [32] were investigated of necessity as hybrid mixtures in the presence of the parent species [41] and either [24] or [23], respectively. Resolution of $O_2$ binding free energies of these species was straightforward on the basis of the following strategy. Figure 6 shows the fraction of sites capable of binding $O_2$ [i.e., the Fe(II) heme sites] on the various dimeric and tetramer forms in the mixture as a function of the proportion of initial parent species [41]. At the upper asymptotic limit of species [41] the shape and position of the $O_2$ binding isotherm of the hybrid mixture is dominated by species [32]. This strategy is possible because one of the parent species, [41], does not bind $O_2$.

Thus, the data were analyzed according to eq A5 while constraining the previously determined values for the species [23] dimer and tetramer $O_2$ binding free energies without concern for inducing bias error. Similarly, the dimer–tetramer assembly free energy of the fully-oxygenated form of species

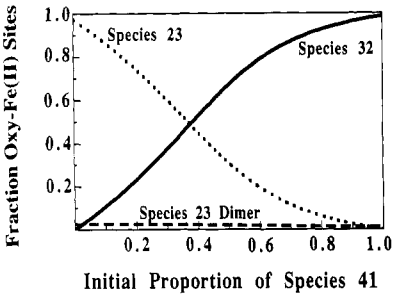


FIGURE 6: Fraction of Fe(II) heme sites which exist as species [32] versus the proportion of species [41] parent molecule. Conditions are given in Figure 7. Total Hb concentration was 1.85 mM heme. Curves were generated with experimentally determined equilibrium constants for the fully-oxygenated system.

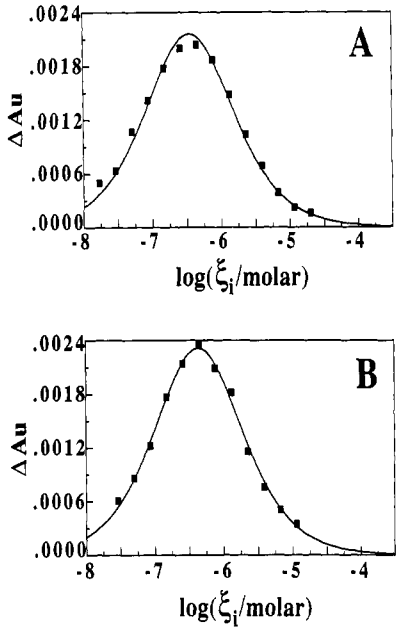


FIGURE 7: Derivative $O_2$ equilibrium isotherms (at 415 nm) for (A) species [31] (in mixture with [24] and [41]) and (B) species [32] (in mixture with [23] and [41]). Conditions: 0.1 M Tris, 0.1 M NaCl (0.18 M total chloride), 1 mM $Na_2EDTA$, and 10 $\mu$M KCN, pH 7.40 at 21.5 °C. Initial heme concentrations of parent species were as follows: (A) 1.67 mM species [41] and 0.175 mM species [24] and (B) 1.67 mM species [41] and 0.195 mM species [23]. Curves represent nonlinear regression to eq 5. The square root of the variance was ($\bar{Y}$ units) 0.0048 (A) and 0.0034 (B).

[32] (Figure 8, determined by cryogenic isoelectric focusing) was constrained during regression. The resolved $O_2$ binding free energies were insensitive to tenths of a kilocalorie perturbation in the constrained assembly free energies, so that regression analysis according to eq 5 was for practical purposes a two-parameter problem ($\Delta A_T$ and a single $O_2$ binding equilibrium constant for species [32]). Figure 7 shows the $O_2$ equilibrium data, and Figure 8 and Table I summarize the results of the regression analysis. The $O_2$ binding free energies of both species [31] and [32] are seen to be extremely favorable (even more favorable than the dissociated constituent dimers).

The dimer–tetramer assembly free energies for cyanomet species [31] and [32] (Figure 8) were determined by conservation of energy from $O_2$ binding free energies of the tetramers, $O_2$ binding free energies of the constituent dimers (determined for species [23] and [24], above), and dimer–tetramer assembly free energies of the fully-oxygenated forms of cyanomet species [31] and [32] from cryogenic isoelectric focusing experiments. The reported assembly free energies of [31] and [32] agree, within error, with the values of −8.00 ± 0.2 and −8.14 ± 0.2 kcal, respectively, determined by

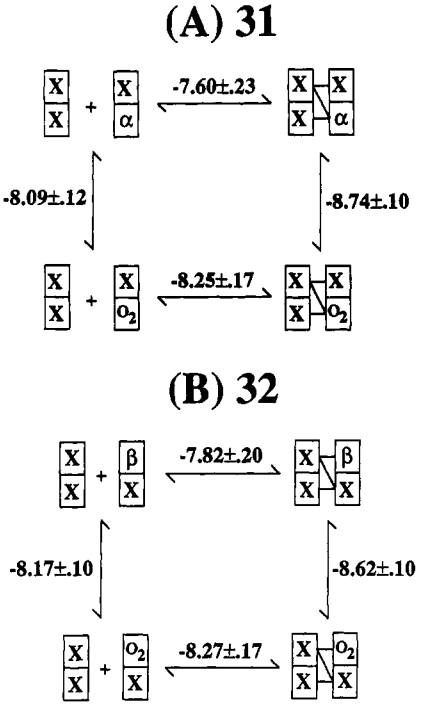


FIGURE 8: Thermodynamic linkage between subunit assembly and $O_2$ binding to the triply-ligated cyanomet species [31] and [32]. The ligand cyanomet is denoted by X. Orientation of $\alpha$ and $\beta$ subunits within the dimer and tetramer is indicated in the deoxy species. Conditions are given in Figure 7.

Table II: Kinetics for Reacting Free Sulfhydryl Groups with 4-PDS on Isolated Ligation Species of Hb and Hybrid Mixtures (Assignments Discussed in Text)[a]

| | 21.5 °C | | other temperatures | | |
|---|---|---|---|---|---|
| species | method | half-life (s) and amplitude (%) | method | half-life (s) and amplitude (%) | temp (°C) |
| [01] | split cell | 240 (100) | split cell | 184 (100) | 30 |
| [11] | n.d. | | stopped flow | 9 (31) | 28 |
| | | | | 46 (14) | |
| | | | | 550 (55) | |
| [12] | n.d. | | stopped flow | 6 (36) | 29 |
| | | | | 67 (16) | |
| | | | | 350 (48) | |
| [21] | split cell | 10 (17) | stopped flow | 1.1 (7) | 25 |
| | | 132 (8) | | 13 (44) | |
| | | 724 (30) | | 57 (9) | |
| | | | | 660 (40) | |
| [22] | split cell | 14 (26) | n.d. | | |
| [23] | split cell | 11 (48) | split cell | 5 (12) | 30 |
| | | 85 (8) | | 79 (20) | |
| [24] | split cell | 13 (62) | split cell | 6 (18) | 30 |
| | | 102 (17) | | 72 (27) | |
| [31] | split cell | 13 (55) | n.d. | | |
| [32] | split cell | 11 (40) | n.d. | | |
| [41] ($O_2$) | split cell | 6 (34) | split cell | 6 (44) | 30 |
| [41] (CN) | split cell | 7 (34) | n.d. | | |

[a] Conditions as in Figure 3 with 600 $\mu$M 4-PDS and 40 $\mu$M total heme. n.d., not determined.

cryogenic isoelectric focusing (Daugherty and Ackers, manuscript in preparation).

*Kinetics of Reacting Free Sulfhydryl Groups.* Table II summarizes the kinetics for reacting free sulfhydryls on each of the 10 cyanomet ligation states. The kinetic parameters given for four of the species refer exclusively to a single ligation state studied in isolation (species [01], [23], [24], and [41]), while the values listed for the remaining species reflect behavior of the hybrid mixtures. The relative initial concentrations of the parents in the hybrid cases were approximately 1:1, so

that the resulting relative concentrations of the three types of tetramers at equilibrium were approximately 1:2:1 [(parent AA):(hybrid AB):(parent BB), where A and B represent unique $\alpha\beta$ dimers]. For example, species [11] was created by mixing species [01] and [23]. The observed kinetics therefore reflect the three tetramers, [01], [11], and [23], plus contributions from the dissociated $\alpha\beta$ dimers (which are present at approximately 5% of the total heme concentration in the case of the hybrid mixture containing species [11]). Temperatures listed for the stopped-flow determinations correspond to ambient values inside the anaerobic chamber. Relative error on half-lives (Table II) is 5–10% based on regression analysis.

Because many of the ligation species had to be studied as hybrid mixtures, a complete molecular interpretation of the kinetics listed in Table II was not attempted. Assignment of the observed kinetics in these instances is further complicated by the factor that multiple allosteric forms may be accessible to each species (each with distinct sulfhydryl reactivities), and multiple sulfhydryl reactivities are possible for a given allosteric form. Thus, while some of the kinetic half-lives listed in Table II may be assigned to particular molecular species, others represent upper limits.

Nevertheless, several conclusions are clear from the trends in these data (Table II). (1) A 35-fold change in kinetic behavior was found between deoxy Hb and fully-cyanomet (or equivalently fully-oxy) Hb. The kinetics of these end-state Hbs were very well described by single first-order processes. (2) Nearly identical patterns of sulfhydryl reaction kinetics were observed for the hybrid mixtures containing species [11], [12], and [21]. They each required a minimum of three exponentials to describe the data (species [21] required a fourth very fast phase in the stopped-flow experiment), and in all three cases approximately half of the amplitude change originated from a very long kinetic phase. Since this long kinetic phase cannot originate from any of the parent species (on the basis of the independently determined kinetics of the parents studied in isolation), it must correspond to the hybrid tetramers [11], [12], and [21]. (3) In contrast, the sulfhydryl reaction kinetics of species [22], [23], [24], [31], and [32] were all rapid. The two species that could be studied in isolation, [23] and [24], each required a minimum of two exponentials, although the longer phase in each case made a minor contribution to the overall kinetics. When studied in hybrid mixtures, species [22], [31], and [32] were well-described by a single exponential. The ability to describe the hybrid mixtures containing species [22], [31], and [32] with a single exponential is due in part to the long dead time of the split cell method (10–15 s) and the general problems of resolving multiple exponentials that have similar half-lives. Regardless of these complexities, an upper limit half-life of approximately 15 s could clearly be assigned to the three hybrid tetramers.

The present results are consistent with initial-rate studies of the reactions of 4-PDS with Hb at intermediate $O_2$ partial pressures (Makino & Sugita, 1982) in that a minimum of four molecular species were required to accommodate the data. Makino and Sugita found, however, that the triply-oxygenated species reacted with a faster initial rate than the fully-oxygenated species, whereas our results are suggestive of the converse. These differences are not inconsistent given that initial rates were evaluated in their work and overall rates were measured in the present study.

## DISCUSSION

*Cooperative Mechanism of Cyanomet Ligation of Hb.* The cooperative mechanism of Hb is manifested as the energetic couplings between the 10 tetrameric microstates (Figure 1) and their relation to tertiary and quaternary structural transitions. Measurement of these couplings for all tetrameric species has been possible with the nonlabile heme-site ligand cyanomet, in combination with subunit assembly methods which exploit conservation of energy between subunit assembly and heme-site ligation. Early studies revealed a large asymmetry between the cooperative energetics of species [21] versus the other doubly-ligated species (Smith & Ackers, 1985), indicating a combinatorial aspect to cooperativity. More recent studies by Daugherty et al. (1991) on the effects of mutational perturbation and proton coupling have permitted assignment of the quaternary structure of species [21] as deoxy T. This assignment, in conjunction with the observed energetic distributions, implicated a "symmetry rule" for heme-site ligation induced quaternary structure change [i.e., the crystallographically-defined rotation of the $\alpha^1\beta^1$ dimer relative to the $\alpha^2\beta^2$ dimer [cf. Baldwin and Chothia (1979)]]. That is, the T $\rightarrow$ R quaternary change is governed by the ligation steps which lead to a tetramer with at least one occupied heme site on each side of the $\alpha^1\beta^2$ interface (Figure 1).

Further studies on the ligation microstates of Hb, including experimental results on several other heme-site ligation systems, have led to a more comprehensive molecular "code" for cooperativity (Ackers et al., 1992). The symmetry rule for T $\rightarrow$ R quaternary switching plays a fundamental role in this code, as do cooperative interactions within each of the T and R quaternary structures (i.e., tertiary interactions). Here we summarize the molecular code as a tetrameric partition function. This "consensus" partition function is based on the common patterns of cooperative behavior observed with a variety of ligation systems and represents the dominant allosteric forms that are experimentally detected.

$$\Xi(X) = 1 + 2K_{tc}(K_\alpha + K_\beta)X + (2K_\alpha K_\beta K_{tc}^{21} + 2K_\alpha K_\beta K_C K'_{tc} + K_\alpha{}^2 K_C K'_{tc} + K_\beta{}^2 K_C K'_{tc})X^2 + 2K_C K'_{tc}(K_\alpha K_\beta{}^2 + K_\alpha{}^2 K_\beta)X^3 + K_\alpha{}^2 K_\beta{}^2 K_C X^4 \quad (9)$$

$K_\alpha$ and $K_\beta$ are intrinsic binding constants for the $\alpha$ and $\beta$ subunits. The remaining equilibrium constants reflect the following tetrameric cooperative interactions. $K_{tc}$ is a "tertiary constraint" interaction constant for the first ligation event that corresponds to the "mismatch" situation of having a subunit with ligated tertiary structure within the T quaternary structure. Similarly, $K_{tc}^{21}$ denotes the tertiary constraint for the formation of species [21] within the T structure. $K'_{tc}$ is a tertiary constraint constant reflecting the mismatch due to having an unligated tertiary structure(s) within the R quaternary structure. $K_C$ is the product of all cooperative interaction constants for the binding of four ligands onto the tetramer. It corresponds to the total cooperative free energy, $^{41}\Delta G_c$. The relationship between eq 9, which explicitly accounts for the cooperative energetics of every ligation microstate, and $O_2$ equilibrium measurements, which only probe the stoichiometric macroscopic ligation states, is described below.

We note that under certain solution conditions, such as in high salt or in the presence of potent allosteric effectors, it may be possible to populate allosteric species not considered in eq 9. For instance, organic phosphates may thermodynamically drive species [23] and [24] from predominantly quaternary R toward quaternary T (Ogawa & Schulman, 1972; Maeda et al., 1972; Nagai, 1977). Thus, in the presence of organic phosphates additional terms would be required in the partition function. Since a complete accounting of accessible states would include the contributions from all 10

ligation species in both R and T quaternary forms, a more detailed understanding of the molecular underpinnings of cooperativity is possible from studies as a function of the chemical potential of allosteric effectors and/or temperature.

*Implications of the $O_2$ Binding Energetics and Sulfhydryl Kinetics for the Cooperative Mechanism.* The pattern of $O_2$ affinities for the cyanomet microstates (Table I) strongly supports the distribution of cooperative free energies obtained previously (Daugherty et al., 1991). For example, the overall $O_2$ affinity (indicated by the free energy per site) is lower for species [21] than for the species [22], [23], and [24] by approximately 1.5 kcal/mol. This considerable difference in overall $O_2$ affinities of the doubly cyanomet-ligated molecules clearly discriminates against the classical two-state concerted model (Monod et al., 1965) for cooperative cyanomet ligation (Ackers, 1990). Previous work, which employed cyanomet species [23] and [24] as models for the $O_2$-bound species [23] and [24], showed that the combined data base of $O_2$ binding to the vacant heme sites on cyanomet species [23] and [24] together with the $O_2$ binding equilibria of normal Hb was incompatible with the two-state concerted model, even allowing for $\alpha$ and $\beta$ subunit heterogeneity (Minton, 1974). The present study delineates the failure of the two-state model in that the last two $O_2$ binding steps of normal Hb are not well-described by $O_2$ binding to cyanomet species [23] and [24], but are instead influenced by a weighted average of the highly asymmetric $O_2$ binding properties of those species (and species [22]) versus species [21].

The cooperativities of the doubly-ligated species also differ widely, as measured by the maximum Hill slopes of their isotherms. The considerable Hill slope of 1.94 for species [21] is close to the theoretical maximum of 2 for a two-site case, while the remaining double-ligated species show minimal Hill slopes near 1.2. Thus, the $O_2$ affinities and cooperativities for filling the vacant heme sites on the doubly cyanomet-bound species are consistent with the concept that species [21] is predominantly quaternary T, whereas the high $O_2$ affinities and low cooperativities of species [22], [23], and [24] are indicative of molecules predominantly in quaternary R. The cooperativity observed upon oxygenation of cyanomet species [23] and [24] would thus correspond to sequential cooperativity driven by tertiary interactions within quaternary R.

In the present study we also correlate changes in sulfhydryl reactivity of the 10 cyanomet microstates with the predicted changes in quaternary and tertiary structure outlined by the partition function eq 9. The kinetics of reacting free sulfhydryls with a reagent such as 4-PDS is in principle a local probe of structure, reflecting only the chemical environment surrounding a given residue (or small number of residues). Therefore, sulfhydryl reaction studies alone are incapable of distinguishing between tertiary and quaternary structure changes. In human Hb the reactive sulfhydryl group has been identified as $\beta$93 Cys (Guidotti & Konigsberg, 1964). The close proximity of $\beta$93 Cys to the $\alpha^1\beta^2$ interface suggests that changes in sulfhydryl reaction kinetics will be governed in large part by the T → R quaternary structure change (Perutz et al., 1974), but tertiary structure changes have also been implicated as controlling factors in sulfhydryl reactivity (Guidotti, 1965; Perutz et al., 1974). The present investigation provides at the same time a consistency test of the proposed molecular code (eq 9) and a data base for evaluating the contributions of quaternary and tertiary structure change upon sulfhydryl reactivity in Hb.

The pattern of kinetics for reacting the free sulfhydryl groups on each of the 10 microstates (Table II) strongly supports the symmetry rule for quaternary structure change. In particular, we observed a long kinetic phase ($t_{1/2} \approx 500$ s) attributable exclusively to species [11], [12], and [21], whereas a dramatic increase in reaction rate was observed for those species which have at least one ligand on both sides of the $\alpha^1\beta^2$ interface. Less drastic (2-fold) changes in the rates of sulfhydryl reactivities of species [01] compared to species [11], [12], and [21] are consistent with smaller, tertiary structure changes within the T quaternary structure. Similarly, 2-fold changes in the reactivities of species [41] compared to species [22], [23], [24], [31], and [32] are consistent with tertiary structure changes occurring within the R quaternary structure.

Table III: Cooperative Free Energies, ${}^{ij}\Delta G_c$, for Microstate Intermediates of Several Heme-Site Ligation Systems of Hb[a]

| microstate species [ij] | Fe(II)/ Fe(III)–CN[b] | Fe(II)/ Fe(III)–CN[c] | Fe(II)/ Fe(II)–$O_2$[d] | Co(II)/ Fe(II)–CO[e] | Co(II)/ Co(II)–$O_2$[f] |
|---|---|---|---|---|---|
| [01] | 0 | 0 | 0 | 0 | 0 |
| [11] | 3.14 | 2.85 | 2.9 | 1.5 | 1.9 |
| [12] | 3.42 | 3.15 | 2.9 | 2.0[e] | 1.9 |
| [21] | 3.01 | 3.15 | 5.1 | 2.1 | 2.9 |
| [22] | 6.68 | 6.05 | 7.1 | 3.0[e] | 2.3 |
| [23] | 6.43 | 6.15 | 7.1 | 3.1 | 2.3 |
| [24] | 6.51 | 5.85 | 7.1 | 3.2 | 2.3 |
| [31] | 6.95 | 5.75 | 7.1 | 3.0 | 2.3 |
| [32] | 6.75 | 5.80 | 7.1 | 3.1 | 2.3 |
| [41] | n.a. | 5.90 | 6.3 | 2.6 | 1.8 |

[a] Conditions as in Figure 3. Species [ij] designations given in Figure 1. See text for calculation of ${}^{ij}\Delta G_c$. Typical precision is ±0.2 kcal. [b] This study. "Penalties" for $O_2$ binding to vacant heme sites on species [ij] were used with the total cooperative free energy (6.3 kcal) to determine the ${}^{ij}\Delta G_c$ spent in the formation of cyanomet species [ij] (see eq 11). [c] Smith & Ackers, 1985; Perrella et al., 1990a. Cyanomet species [ij] ${}^{ij}\Delta G_c$ determined from subunit assembly measurements. [d] Doubly-oxygenated values are predicted from the molecular code of Ackers et al. (1992) and $O_2$ binding data (Chu et al., 1984). Singly- and triply-oxygenated species are composite $\alpha$ and $\beta$ isomer values. Error on the [21] value is approximately ±1.5 kcal. [e] Speros et al., 1991. ${}^{ij}\Delta G_c$ values for species [12] and [22] were poorly resolved (±0.4 kcal). Errors on the other species were ±0.2 kcal. [f] Predictions based on the molecular code of Ackers et al. (1992) and $O_2$ binding data (Doyle et al., 1991). Dimers are assumed noncooperative.

*Determination of the Cooperative Free Energy Distribution of Cyanomet Microstates from $O_2$ Binding Measurements.* $O_2$ binding has been used in the present study to probe the energetics of the cyanomet distribution. Table III gives the distributions of microstate energetics for several heme-site ligation systems that exemplify the range of cooperative behavior observed in Hb. The tabulated values are cooperative free energies ${}^{ij}\Delta G_c$, corresponding to the free energy "spent" by the tetrameric molecule during formation of species [ij] from species [01]. The equilibrium constant ${}^{ij}K$ for binding $i$ ligands to form species [ij] is therefore

$$ {}^{ij}K = K_x^i \exp(-{}^{ij}\Delta G_c/RT) \qquad (10) $$

$R$ is the gas constant, $T$ is absolute temperature, and $K_x^i$ is a product of $i$ intrinsic ligand binding constants pertaining to the specific combination of $\alpha$ and/or $\beta$ subunit(s) ligated in the formation of species [ij] [see Ackers (1990) and Doyle et al. (1991) for more detailed forms of this equation].

Cooperative free energies were determined in the present study from $O_2$ equilibrium measurements according to

$$ {}^{ij}\Delta G_c = 6.3 + (\sum {}^{ij}\Delta G_{O_2}^{dimer} - {}^{ij}\Delta G_{O_2}^{tetramer}) \qquad (11) $$

where ${}^{ij}\Delta G_{O_2}^{tetramer}$ is the measured $O_2$ binding free energy for filling all vacant heme sites on tetrameric species [ij]. The sum of relevant dimeric $O_2$ binding free energies for species [ij], $\sum {}^{ij}\Delta G_{O_2}^{dimer}$, represents the intrinsic, reference state of the

subunits and varies slightly among microstate species depending on the number and position of cyanomet ligands bound to the dissociated dimers. The 6.30 ± 0.2 value in eq 11 is the total free energy penalty which opposes binding of four oxygens onto the unligated species [01] (Chu et al., 1984).

The difference between the tetramer and dimer $O_2$ binding free energies described by eq 11 is a measure of the energetic "penalty" for binding $O_2$ to the tetramer relative to the noncooperative dimer. The cooperative free energy "spent" in the formation of cyanomet species [*ij*] is the difference between the measured penalty for $O_2$ binding to the vacant heme sites on species [*ij*] versus the total penalty for complete oxygenation (6.3 kcal) and thus reflects the amount of cooperative free energy remaining in the tetramer after cyanomet species [*ij*] has been formed. $O_2$ equilibrium measurements are therefore used in the present study as a means of probing the cooperative energetics of the cyanomet distribution.[3]

Cooperative free energies of cyanomet ligation are also determinable from dimer–tetramer assembly measurements (Smith & Ackers, 1985; Perrella et al., 1990a) since cooperative free energy is a property of the entire tetramer molecule independent of path. The small differences between cooperative free energies determined here and those determined previously (columns 1 and 2, Table III) originate from the small "scaling" difference between the overall cooperative free energy for $O_2$ ligation (6.3 ± 0.2 kcal) versus cyanomet ligation (5.9 ± 0.2 kcal) and the slight asymmetry in the intrinsic $O_2$ equilibrium constants for $\alpha$ and $\beta$ subunits of the dissociated singly cyanomet-ligated dimers accounted for in the present study.

*Predicted Microstate Cooperative Free Energies of $O_2$.* Cooperative free energies for the oxygenated intermediates in Table III (columns 4 and 6) are not experimental measurements per se, since $O_2$ equilibrium measurements are incapable of distinguishing between microstate isomers at a given stoichiometry of binding. On the other hand, there is good reason for assigning these ${}^{ij}\Delta G_c$ values on the basis of $O_2$ equilibrium data using the consensus partition function eq 9 as a model.

The ${}^{ij}\Delta G_c$ values for the singly-oxygenated species can be determined experimentally as the composite value for the $\alpha$ and $\beta$ isomers (species [11] and [12]) from dimer–tetramer assembly and $O_2$ equilibrium measurements. This quantity is equal to the difference between the $O_2$ binding free energies of the first binding steps of the tetramer and the dimer [cf. Mills et al. (1976)]. In view of the symmetry in the ${}^{ij}\Delta G_c$ values of species [11] and [12] for the nonlabile heme-site ligands (to within a few tenths of a kilocalorie) it is reasonable to partition the measured composite cooperative free energy equally to species [11] and [12], as given in Table III. Furthermore, within either the iron or cobalt ligation systems, the magnitudes of the composite ${}^{ij}\Delta G_c$ values for $O_2$ at the first step are very similar to those of the intrinsic nonlabile cases. Equivalence of species [11] and [12] is denoted in the partition function eq 9 by a single term ($K_{tc}$).

Similarly, the composite ${}^{ij}\Delta G_c$ of $\alpha$ and $\beta$ isomers at the triply-oxygenated state is well-determined from measurements of $O_2$ binding and dimer–tetramer assembly equilibria (calculated as the total cooperative free energy minus the difference between the $O_2$ binding free energies of the last binding steps of the tetramer and the dissociated dimer). Since there is only slight asymmetry in the cooperative free energies of the $\alpha$ and $\beta$ isomers at the triply-ligated states of the nonlabile heme-site ligation systems, it is reasonable again to assign equally the measured composite cooperative free energy to species [31] and [32]. In the partition function eq 9 these species are weighted by the same combination of cooperative interaction terms ($K_C K'_{tc}$).

In view of the considerable asymmetry between the cooperative energetics of the microstate isomers at the doubly-ligated level (as determined with the nonlabile ligand systems, Table III), assignments of cooperative free energies to the double-oxygenated microspecies relies somewhat more upon the consensus partition function. The composite cooperative free energy over all doubly-oxygenated microstates can be determined experimentally from $O_2$ equilibrium and subunit assembly measurements and is equal to the difference between the composite dimer–tetramer assembly free energy over all doubly-oxygenated species and the assembly free energy of species [01]. For the case of noncooperative dissociated dimers, this composite dimer–tetramer assembly constant, $\overline{K_2}$, is related to the microstate species assembly equilibria as (Ackers & Halvorson, 1974; Doyle et al., 1991)

$$\overline{K_2} = 2\,{}^{21}K_2 + 2\,{}^{22}K_2 + {}^{23}K_2 + {}^{24}K_2 \qquad (12)$$

Here ${}^{2j}K_2$ is the intrinsic dimer–tetramer assembly equilibrium constant for microstate species [2*j*]. Cooperative free energies of the double-oxygenated microstates in Table III were predicted according to the consensus partition function eq 9 in combination with experimentally determined values of $\overline{K_2}$ for $O_2$. Cooperative free energies of the $O_2$ microstate species [22], [23], and [24] were assumed to be the same as the experimentally determined composite intrinsic value at the triply-oxygenated state (i.e., weighted by the same product of cooperative interaction constants in eq 9, $K_C K'_{tc}$). The cooperative free energy for species [21] was then calculated from eq 12 as ${}^{21}\Delta G_c = -RT \ln ({}^{21}K_2/{}^{01}K_2)$, where ${}^{01}K_2$ is the dimer–tetramer assembly equilibrium constant for the unligated species [01].

The microstate distributions predicted by eq 9 from $O_2$ equilibrium data (Table III, columns 4 and 6) are highly consistent with the experimentally determined microstate distributions of the nonlabile heme-site ligands. This is particularly evident for the singly- and triply-ligated species for both ferrous and cobaltous Hb. Consistency is also present at the doubly-ligated level, but with a large degree of uncertainty originating from the $O_2$ equilibrium data.

*Comparison with Microstate Distributions of Other Heme-Site Ligands.* Inspection of the cooperative free energies for the various ligation systems in Table III reveals features that are common to all of the systems. Quantitative manifestations may, however, vary between ligation systems and as a function of solution conditions. The Co(II)/Fe(II)–CO system portrays clearly the most general pattern of cooperative interactions, showing a free energy distribution in accord with the symmetry rule, quaternary enhancement for species [22], [23], [24], [31], and [32] versus species [41] (i.e., whenever ${}^{ij}\Delta G_c > {}^{(i+1)j}\Delta G_c$; see also discussion below), and differences between the cooperative free energies of species [11], [12], and [21]. In the case of the Fe(II)/Fe(III)–CN system, the symmetry rule and quaternary enhancement are clearly represented, while differences between the cooperative free energies of species [11], [12], and [21] are not as pronounced as in the Co(II)/Fe(II)–CO system.

[3] Conversely, if it were experimentally feasible to isolate the eight oxygenated microstates and measure cyanomet binding equilibria to their vacant sites, the resulting free energy penalties for cyanomet ligation would probe the cooperative free energies of the oxygen microstates. Values of these free energies listed in Table III (as predicted by constraining the stepwise oxygen equilibrium results by the consensus partition function) are thus not in conflict with the quantitatively different distributions listed for the cyanomet cooperative free energies.

Microstate distributions of two other heme-site ligation systems [Fe(II)/Mn(III) and Mn(II)/Fe(II)–CO] have been discussed by Smith et al. (1987) and by Ackers (1990). Both of these ligation systems have cooperative energetics that clearly portray the symmetry rule.

*Quaternary Enhancement as a Source of Regulatory Energy at High Fractional Saturation.* The overall effect of assembly of the isolated $\alpha$ and $\beta$ subunits (or $\alpha\beta$ dimers) into $\alpha_2\beta_2$ tetramers is to oppose (or constrain) $O_2$ binding. However, cooperativity in Hb is accomplished by successive release of quaternary constraint energy at low fractional saturations and the gain of quaternary enhancement energy at high fractional saturations (Mills & Ackers, 1979a). Quaternary enhancement is typically manifested as a higher ligand affinity at the last binding step of the tetramer than that of a $\alpha\beta$ dimer (or, by conservation of energy, a less favorable dimer–tetramer assembly free energy at the third tetrameric ligation state as compared to the fourth). Early observations that the $O_2$ affinity at the fourth binding step of tetrameric Hb exceeds that of the dissociated monomeric subunits were reviewed by Baldwin (1975). This effect was also reported by Imai and Yonetani (1975), and by Di Cera et al. (1987). Szabo and Karplus (1972) found that their mathematical model, when fit to the classical oxygenation data of Roughton and Lyster (1965), led to an $O_2$ affinity at the last tetrameric step that was higher than the intrinsic subunit value.

The phenomenon of quaternary enhancement is closely related to that of cooperativity within the quaternary R tetramer. If quaternary enhancement were to exist only at the fourth binding step, the tetrameric species could in principle operate as a two-state MWC system where the R-state molecules have no cooperativity (Ackers & Johnson, 1981). If however, any of the R-state doubly-ligated species also exhibit quarternary enhancement (e.g., species [22], [23], [24]) then cooperativity will be manifested at the last two binding steps of those species. In a recent study on the ligation species of the cobaltous/iron–CO Hb system (Speros et al., 1991) it was found that species [23], [24], [31], and [32] all exhibited 0.5 kcal of quaternary enhancement. This result provides justification for the tetrameric R-state cooperativity term $K'_{tc}$ in the consensus partition function, eq 9.

The existence of quaternary enhancement in Hb has recently been questioned (Gibson & Edelstein, 1987; Philo & Lary, 1990), on the basis of a discrepancy between kinetically derived estimates of the last $O_2$ binding equilibrium constant and those determined from regression analysis of $O_2$ equilibrium curves [see Ackers and Johnson (1990) for review]. Much experimental information which bears on the issue of quaternary enhancement has been gained since this "kinetic-versus-equilibrium" discrepancy was reported, including results from the present study. A summary is given in Table IV of quaternary enhancement energies measured under the same conditions on a range of human Hb ligation systems and with a variety of experimental methods. The combined data base represented by Table IV presents a strong case for the existence of quaternary enhancement in Hb, the magnitude of which is seen to vary somewhat between ligation systems.

Quaternary enhancement at the fourth $O_2$ binding step of Hb can be measured most directly from the $O_2$ equilibrium data on species [31] and [32] (Figure 7). The tetrameric $O_2$ binding free energies reported in Figure 8 are for practical purposes direct measurements since they were determined from isotherms that reflected essentially pure hybrid species [31] and [32] (see Figure 6), although rigorous equations including dissociated dimers and parent species, [41] and either [24] or [23], were used in the analysis (eq A5). The average quaternary enhancement free energy for binding $O_2$ to triply-cyanomet Hb was found to be 0.55 kcal, or an enhancement factor of 2.7 on the $O_2$ binding equilibrium constant of the tetramer relative to the dimer.

Table IV: Experimental Measurements of Quaternary Enhancement Energies in Human Hb at pH 7.4, 21.5 °C, 0.1 M Tris, 0.1 M NaCl, and 1 mM $Na_2EDTA$

| Hb system | quaternary enhancement energy (kcal) | reference |
|---|---|---|
| normal Hb | 0.81 (±0.27)/$O_2$ | Mills & Ackers, 1979a |
| normal Hb[a] | 0.94 (±0.22)/$O_2$ | Mills & Ackers, 1979b |
| normal Hb[b] | 0.88 (±0.10)/$O_2$ | Chu et al., 1984 |
| recombinant Hb $\beta$1 Val → Ala | 1.13 (±0.37)/$O_2$ | Doyle et al., 1992a |
| recombinant Hb $\beta$1 Val → Met | 0.47 (±0.50)/$O_2$ | |
| recombinant Hb $\beta$1 plus Met | 0.63 (±0.57)/$O_2$ | |
| Hb Ypsilanti ($\beta$99 Asp → Tyr) | 2.60 (±0.14)/4 $O_2$ | Doyle et al., 1992b |
| $\beta_4$ tetramer | 3.38 (±0.60)/4 $O_2$ | Valdes & Ackers, 1978 |
| cobaltous Hb | 0.48 (±0.12)/$O_2$ | Doyle et al., 1991 |
| Co(II)/Fe(II)–CO | 0.52 ± 0.09)/Fe(II)–CO | Speros et al. 1991 |
| cyanomet [31][c] | 0.65 (±0.16)/$O_2$ | this study |
| cyanomet [32] | 0.45 (±0.14)/$O_2$ | |
| cyanomet [23] | 0.33 (±0.12)/last $O_2$ | |
| cyanomet [23] | 0.13 (±0.11)/2 $O_2$ | |
| cyanomet [24] | 0.37 (±0.14)/last $O_2$ | |
| cyanomet [24] | 0.21 (±0.20)/2 $O_2$ | |

[a] Average from $O_2$ binding isotherms measured from 10 to 37 °C. [b] Average from $O_2$ binding isotherms measured from pH 7.4 to 9.5. [c] See Figure 1 for species [*ij*] designations.

Quaternary enhancement is also clearly seen at the last step in the $O_2$ binding studies of cyanomet species [23] and [24] (Figure 5), where the average quaternary enhancement energy is 0.33 kcal. The overall quaternary enhancement energy between the deoxygenated and fully oxygenated forms of species [23] and [24] is small (perhaps two-tenths of a kilocalorie). A similar magnitude is found for cyanomet ligation of these species, i.e., without any $O_2$ binding (Daugherty and Ackers, manuscript in preparation). Although this latter effect approaches the measurement noise level at any single set of conditions, its constancy over the pH range 7.4–9.5 indicates that it is real.

*Ligand Binding to $\alpha\beta$ Dimers as the Protomeric Reference State.* Cooperative free energies in multisubunit macromolecules may be decoupled from the intrinsic ligand binding free energies of the protomeric subunits by investigations of the thermodynamic linkage between subunit assembly and ligand binding (Ackers & Halvorson, 1974; Turner et al., 1992). For example, there is a large degree of cooperativity for cyanomet ligation within the $\alpha\beta$ half-molecules of tetrameric Hb, the difference between the first and second ligation free energies being 3 kcal (Smith & Ackers, 1985). Yet, the interactions responsible for this cooperativity are lost upon dissociation of the tetramer into dimers since $O_2$ binding to the dissociated $\alpha\beta$ dimers shows noncooperative behavior to within 0.1–0.2 kcal (Mills et al., 1976; Chu et al., 1984; Doyle et al., 1992a).

Table V lists the $O_2$ binding free energies of Hb promoters ($\alpha$ and $\beta$ subunits) in the pure monomer and $\alpha\beta$ dimer forms. Determination of the pure monomer binding free energies is based on measurements of the linkage between oxygenation and either $2\alpha \rightarrow \alpha_2$ or $4\beta \rightarrow \beta_4$ subunit assembly (Valdes & Ackers, 1978; Mills et al., 1979). Two main conclusions can be drawn from Table V. First, the $O_2$ binding free energies of the $\alpha$ and $\beta$ subunits within the $\alpha\beta$ dimer are nearly equal (to within a few tenths of a kilocalorie) to the values of the $\alpha$ and $\beta$ monomers. The average change in affinity upon forming the dimer corresponds to 0.45 kcal of quaternary enhancement per $O_2$.

Table V: Protomer $O_2$ Binding Free Energies at pH 7.4 and 21.5 °C

| protomer | $O_2$ binding free energy (kcal) | reference |
|---|---|---|
| $\alpha\beta$ dimer (average of $\alpha$ and $\beta$ subunits)[a] | −8.36 ± 0.10 | Mills et al., 1976; Chu et al., 1984 |
| $\alpha$ monomer | −8.11 ± 0.11 | Valdes & Ackers, 1978; Mills et al., 1979 |
| $\beta$ monomer | −7.71 ± 0.13 | |
| $\alpha$ subunit of $\alpha\beta$ dimer[b] | −8.09 ± 0.12 | this study |
| $\beta$ subunit of $\alpha\beta$ dimer[b] | −8.17 ± 0.10 | |

[a] See also Turner et al. (1992) for review of mutant Hb $\alpha\beta$ dimer $O_2$ binding free energies. [b] The other subunit was cyanomet-ligated.

Second, comparison of the average $O_2$ binding free energy of the $\alpha\beta$ dimer (top row) to the sum of free energies pertaining to the last binding steps of the dimer for the individual $\alpha$ and $\beta$ subunits (bottom two rows) indicates the absence of cooperative interactions within the $\alpha\beta$ dimer, either with the ligand $O_2$ or cyanomet. This noncooperative behavior simplifies use of the $\alpha\beta$ dimers as a reference state in a mathematical sense, although the binding partition function could be extended to include a cooperative dimer as the reference state.

*Chemical Cross-Linking as an Experimental Approach for Studying Allosteric Intermediates.* Rather than study "hybrid" intermediate species as equilibrium mixtures with their parent Hbs, it would seem more direct to chemically cross-link and purify the intermediates. Our initial attempts for measuring directly the $O_2$ binding equilibria of cyanomet species [21] involved cross-linking the two $\alpha\beta$ dimers at their $\alpha$99 lysines with bis(3,5-dibromosalicyl) fumurate. This particular cross-linking reagent was chosen because it yields cross-linked normal Hb with high cooperativity in its $O_2$ binding isotherm (Snyder et al., 1987). We measured the total free energy for binding two oxygens to cross-linked species [21] as −14.6 ± 0.1 kcal, a value well determined but nevertheless in sharp disagreement with −13.4 kcal measured for un-cross-linked species [21] (Table I). Furthermore, the two stepwise intrinsic $O_2$ binding free energies were found to be −7.2 ± 0.4 and −7.4 ± 0.2 kcal/mol of $O_2$, corresponding to an essentially noncooperative isotherm (maximum Hill slope of 1.1). Although this value agrees well with the Hill slope of 1.1 reported for cyanomet species [21] cross-linked at the $\beta$82 lysines with bis(3,5-dibromosalicyl) fumurate (Miura et al., 1987), it is clear that both cross-linked species [21] molecules are altered dramatically in their $O_2$ binding properties with respect to the un-cross-linked species [21].

The discrepancy between $O_2$ binding properties of cross-linked and un-cross-linked species [21] comes as no surprise in view of the delicate energetic balance that is characteristic of allosteric intermediates. Indeed, even noncovalent forces such as the chemical potential of allosteric effector molecules are capable of altering the functional properties of partially-ligated intermediates. Differences in synthesizing high-purity cross-linked samples have also been reported (Shibayama et al., 1991). Thus, although chemical cross-linking is a powerful tool for protein engineering purposes (Snyder et al., 1987), alternative strategies based on unmodified molecules should be sought for accurate structure–function studies whenever possible.

## ACKNOWLEDGMENT

We thank Margaret A. Daugherty and Dr. Paula M. Dalessio for measuring the deviation free energies of the oxygenated forms of cyanomet species [11], [12], [31], and [32] (M.A.D.) and [21] (P.M.D.). We also thank Dr. Francine Smith (University of North Carolina, Chapel Hill) for the cross-linked Fe(II)/Fe(III)–CN species [21].

## APPENDIX

The ligand binding equilibria resolved in the present study are thermodynamically linked to subunit assembly, so that, in the experimental range of Hb concentration studied, special equations are required for correct physical interpretation of the data (Ackers & Halvorson, 1974; Doyle et al., 1986).

Figure 4C depicts the thermodynamic linkage between subunit assembly and oxygenation of tetrameric cyanomet species [23]. The partition function $\Xi(X)$, which includes all macromolecular forms in solution as a function of ligand activity $X$, is written in terms of equilibrium constants with reference to the unliganded dissociated dimer species $[D_{23}]$ as

$$\Xi(X) = [D_{23}]Z_{D23} + [D_{23}]^2\,{}^{23}K_2Z_{23} \qquad \text{(A1)}$$

Oxygen-binding polynomials for tetrameric species [23] and the constituent dimers of species [23] are $Z_{23} = 1 + K_{T1}X + K_{T2}X^2$ and $Z_{D23} = 1 + K_{D1}X$, respectively, where $K_{Ti}$ and $K_{Di}$ are overall equilibrium constants for binding $i$ oxygens to tetramer and dimer forms, respectively. Other nomenclature used throughout this appendix is as follows: ${}^{ij}K_2$ is the intrinsic dimer–tetramer assembly equilibrium constant of species $[ij]$ (corrected for the statistical degeneracy factor of 2 in the cases of species [22], [31], and [32]), $Z_{ij}$ and $Z_{Dij}$ are $O_2$-binding polynomials for tetrameric and dimeric species $[ij]$, $[D_{ij}]$ is the concentration of the deoxygenated form of the constituent dimer of species $[ij]$, and $P_t^{ij}$ is the total concentration of species $[ij]$ in molar heme units. The binding polynomials correspond to the stoichiometric $O_2$ binding equilibrium constants equal in number to heme sites avilable for binding $O_2$ (i.e., the non-cyanomet sites).

In general, the fractional saturation of the system, $\bar{Y}$, is obtained by partial differentiation of the partition function with respect to the logarithm of the $O_2$ activity, normalized to the total concentration of $O_2$ binding sites within the system.

$$\bar{Y} = \frac{\partial\Xi(X)}{(P_t^{23}/2)\partial \ln X} = \frac{[D_{23}]Z'_{D23} + [D_{23}]^2\,{}^{23}K_2Z'_{23}}{(P_t^{23}/2)} \qquad \text{(A2)}$$

Primes on the binding polynomials indicate partial differentiation with respect to the logarithm of $O_2$ activity. The concentration of unliganded dimer $[D_{23}]$ in eq A2 was calculated as the positive quadratic root of the following conservation of mass relation:

$$P_t^{23} = 2\frac{\partial\Xi(X)}{\partial \ln [D_{23}]} = 2[D_{23}]Z_{D23} + 4[D_{23}]^2\,{}^{23}K_2Z_{23} \qquad \text{(A3)}$$

The fractional saturation equation for species [24] was derived in a manner parallel to that of species [23].

However, for the fractional $O_2$ saturation equations for cyanomet species [21], [22], [31], and [32] the situation is more complex due to the fact that these species must be studied as hybrid mixtures in the presence of parent tetramers which also engage in linkages between $O_2$ binding and dimer–tetramer assembly. Here we derive the fractional saturation function for species [32] as an example. The hybrid systems [21], [22], and [31] may then be derived by analogy.

The partition function for the hybrid mixture containing species [32] is

$$\Xi(X) = 2[D_{41}][D_{23}]^{32}K_2Z_{32} + [D_{23}]Z_{D23} + [D_{23}]^2\,{}^{23}K_2Z_{23} + [D_{41}]^2\,{}^{41}K_2 + [D_{41}] \qquad \text{(A4)}$$

Partial differentiation with respect to the logarithm of $O_2$ activity and division by the concentration of total sites available for binding $O_2$ give the fractional saturation.

$$\bar{Y} = \frac{\partial \Xi(X)}{(P_t^{23}/2)\,\partial \ln X} = \frac{[D_{23}]Z'_{D23} + [D_{23}]^{2\ 23}K_2Z'_{23} + 2[D_{41}][D_{23}]^{32}K_2Z'_{32}}{(P_t^{23}/2)} \quad \text{(A5)}$$

The dimer concentrations, $[D_{41}]$ and $[D_{23}]$, in eq A5 were obtained as the simultaneous roots of the following conservation of mass equations.

$$P_t^{23} = 2\frac{\partial \Xi(X)}{\partial \ln [D_{23}]} = 2[D_{23}]Z_{D23} + 4[D_{23}]^{2\ 23}K_2Z_{23} + 4[D_{41}][D_{23}]^{32}K_2Z_{32} \quad \text{(A6)}$$

$$P_t^{41} = 2\frac{\partial \Xi(X)}{\partial \ln [D_{41}]} = 2[D_{41}] + 4[D_{41}]^{2\ 41}K_2 + 4[D_{41}][D_{23}]^{32}K_2Z_{32} \quad \text{(A7)}$$

The roots of eqs A6 and A7 were solved numerically by Newton's iterative method.

## REFERENCES


Ackers, G. K. (1970) *Adv. Protein Chem. 24*, 343–446.
Ackers, G. K. (1990) *Biophys. Chem. 37*, 371–382.
Ackers, G. K., & Halvorson, H. R. (1974) *Proc. Natl. Acad. Sci. U.S.A. 71*, 4312–4316.
Ackers, G. K., & Smith, F. R. (1987) *Annu. Rev. Biophys. Biophys. Chem. 16*, 583–609.
Ackers, G. K., & Johnson, M. L. (1990) *Biophys. Chem. 37*, 265–279.
Ackers, G. K., Doyle, M. L., Myers, D. W., & Daugherty, M. A. (1992) *Science 255*, 54–63.
Ampulski, R. S., Ayers, V. E., & Morell, S. A. (1969) *Anal. Biochem. 32*, 163–169.
Baldwin, J. M. (1975) *Prog. Biophys. Mol. Biol. 29*, 225–320.
Baldwin, J., & Chothia, C. (1979) *J. Mol. Biol. 129*, 175–220.
Benesch, R. E., & Benesch, R. (1962) *Biochemistry 1*, 735–738.
Chu, A. H., Turner, B. W., & Ackers, G. K. (1984) *Biochemistry 23*, 604–617.
Daugherty, M. A., Shea, M. A., Johnson, J., LiCata, V. J., Turner, G. J., & Ackers, G. K. (1991) *Proc. Natl. Acad. Sci. U.S.A. 88*, 1110–1114.
Di Cera, E., & Gill, S. J. (1988) *Biophys. Chem. 29*, 351–356.
Di Cera, E., Robert, C. H., & Gill, S. J. (1987) *Biochemistry 26*, 4003–4008.
Dolman, D., & Gill, S. J. (1978) *Anal. Biochem. 87*, 127–134.
Doyle, M. L., & Ackers, G. K. (1992) *Biophys. Chem. 42*, 271–281.
Doyle, M. L., Gill, S. J., & Cusanovich, M. A. (1986) *Biochemistry 25*, 2509–2516.
Doyle, M. L., Speros, P. C., LiCata, V. J., Gingrich, D., Hoffman, B. M., & Ackers, G. K. (1991) *Biochemistry 30*, 7263–7271.
Doyle, M. L., Lew, G., De Young, A., Kwiatkowski, L., Wierzba, A., Noble, R. W., & Ackers, G. K. (1992a) *Biochemistry 31*, 8629–8639.
Doyle, M. L., Lew, G., Turner, G., Rucknagel, D., & Ackers, G. K. (1992b) *Proteins 14* (Nov issue).
Edsall, J. T., & Gutfruend, H. (1983) in *Biothermodynamics: The Study of Biochemical Processes at Equilibrium*, Wiley & Sons, New York.
Gibson, Q. E., & Edelstein, S. J. (1987) *J. Biol. Chem. 262*, 516–519.
Guidotti, G. (1965) *J. Biol. Chem. 240*, 3924–3927.
Guidotti, G., & Konigsberg, W. (1964) *J. Biol. Chem. 239*, 1474–1484.
Imai, K. (1982) in *Allosteric Effects in Haemoglobin*, Cambridge University Press, London.
Imai, K., & Yonetani, T. (1975) *J. Biol. Chem. 250*, 7093–7098.
Johnson, M. L., & Frasier, S. G. (1985) *Methods Enzymol. 117*, 301–342.
Johnson, M. L., Halvorson, H. R., & Ackers, G. K. (1976) *Biochemistry 15*, 5363–5371.
LiCata, V. J., Speros, P. C., Rovida, E., & Ackers, G. K. (1990) *Biochemistry 29*, 9771–9783.
Maeda, T., Imai, K., & Tyuma, I. (1972) *Biochemistry 11*, 3685–3689.
Makino, N., & Sugita, Y. (1982) *J. Biol. Chem. 257*, 163–168.
Mills, F. C., & Ackers, G. K. (1979a) *Proc. Natl. Acad. Sci. U.S.A. 76*, 273–277.
Mills, F. C., & Ackers, G. K. (1979b) *J. Biol. Chem. 254*, 2881–2887.
Mills, F. C., Johnson, M. L., & Ackers, G. K. (1976) *Biochemistry 15*, 5350–5360.
Mills, F. C., Ackers, G. K., Gaud, H. T., & Gill, S. J. (1979) *J. Biol. Chem. 254*, 2875–2880.
Minton, A. P. (1974) *Science 184*, 577–579.
Miura, S., Ikeda-Saito, M., Yonetani, T., & Ho, C. (1987) *Biochemistry 26*, 2149–2155.
Monod, J., Wyman, J., & Changeux, J. P. (1965) *J. Mol. Biol. 12*, 88–118.
Nagai, K. (1977) *J. Mol. Biol. 111*, 41–53.
Ogawa, S., & Schulman, R. G. (1972) *J. Mol. Biol. 70*, 315–336.
Perrella, M., Benazzi, L., Shea, M. A., & Ackers, G. K. (1990a) *Biophys. Chem. 35*. 97–103.
Perrella, M., Colosimo, A., Benazzi, L., Ripamonti, M., & Rossi-Bernardi, L. (1990b) *Biophys. Chem. 37*, 211–223.
Perutz, M. F., Fersht, A. R., Simon, S., & Roberts, G. C. K. (1974) *Biochemistry 13*, 2174–2186.
Philo, J. S. (1992) *Biophys. J. 61*, A56.
Philo, J. S., & Lary, J. W. (1990) *J. Biol. Chem. 265*, 139–143.
Riggs, A. F. (1952) *J. Gen. Physiol. 36*, 1–16.
Riggs, A. F. (1961) *J. Biol. Chem. 236*, 1948–1954.
Shibayama, N., Imai, K., Hirata, H., Hiraiwa, H., Morimoto, H., & Saigo, S. (1991) *Biochemistry 30*, 8158–8165.
Smith, F. R., & Ackers, G. K. (1985) *Proc. Natl. Acad. Sci. U.S.A. 82*, 5347–5351.
Smith, F. R., Gingrich, D., Hoffman, B. M., & Ackers, G. K. (1987) *Proc. Natl. Acad. Sci. U.S.A. 84*, 7089–7093.
Snyder, S. R., Welty, E. V., Walder, R. Y., Williams, L. A., & Walder, J. A. (1987) *Proc. Natl. Acad. Sci. U.S.A. 84*, 7280–7284.
Speros, P. C., LiCata, V. J., Yonetani, T., & Ackers, G. K. (1991) *Biochemistry 30*, 7254–7262.
Szabo, A., & Karplus, M. (1972) *J. Mol. Biol. 72*, 163–197.
Turner, G. J., Galacteros, F., Doyle, M. L., Hedlund, B., Pettigrew, D. W., Turner, B. W., Smith, F. R., Moo-Penn, W., Rucknagel, D. L., & Ackers, G. K. (1992) *Proteins 14* (Nov issue).
Valdes, R., & Ackers, G. K. (1978) *Proc. Natl. Acad. Sci. U.S.A. 75*, 311–314.
Valdes, R., & Ackers, G. K. (1979) *Methods Enzymol. 61*, 125–141.
Wilhelm, E., Battino, R., & Wilcock, R. J. (1977) *Chem. Rev. 77*, 219–262.
Williams, R. C., & Tsay, K. Y. (1973) *Anal. Biochem. 54*, 137–145.